Effect of coordination number of particle contact force on rutting resistance of asphalt mixture

Niu, Dongyu; Shi, Weibo; Wang, Chen; Xie, Xiwang; Niu, Yanhui

DOI
10.1016/j.conbuildmat.2023.131784

Publication date
2023

Document Version
Final published version

Published in
Construction and Building Materials

Citation (APA)
Niu, D., Shi, W., Wang, C., Xie, X., & Niu, Y. (2023). Effect of coordination number of particle contact force on rutting resistance of asphalt mixture. *Construction and Building Materials*, *392*, Article 131784. https://doi.org/10.1016/j.conbuildmat.2023.131784

Construction and Building Materials 392 (2023) 131784

Contents lists available at ScienceDirect

Construction and Building Materials

journal homepage: www.elsevier.com/locate/conbuildmat

Effect of coordination number of particle contact force on rutting resistance of asphalt mixture

Dongyu Niu [a,b,*], Weibo Shi [a,b], Chen Wang [c], Xiwang Xie [d], Yanhui Niu [a,b,*]

[a] Engineering Research Center of Transportation Materials of the Ministry of Education, Chang'an University, Xi'an 710061, China
[b] School of Materials Science and Engineering, Chang'an University, Xi'an 710061, China
[c] Section of Pavement Engineering, Department of Engineering Structures, Faculty of Civil Engineering and Geosciences, Delft University of Technology, Stevinweg 1, 2628 CN Delft, The Netherlands
[d] State Key Laboratory of High-Performance Civil Engineering Materials, Jiangsu Sobute New Materials Co. Ltd, China

ARTICLE INFO

Keywords:
Road engineering
Asphalt mixture
Skeleton structure
Rutting resistance
Digital image technology
Mann-Whitney *U* test

ABSTRACT

Optimizing asphalt mix design at the indoor stage is of significant importance for enhancing the rutting resistance of asphalt mixture, which is affected by its structural characteristics. In this work, the coordination number of particle contact force (CN_{pcf}) was proposed as an indicator to represent contact characteristics of skeleton structure aggregates in asphalt mixture. Nine asphalt mixtures with different gradations were designed, and the relationship of CN_{pcf} with the number of aggregate contact zones (*CZ*) was established by combining rutting tests and digital image processing technique (DIP). The Mann-Whitney *U* test was implemented to analyze the distribution properties of inter-particle contacts before and after the rutting test. In addition, the resistance to the further expansion of rutting was analyzed. The results revealed a significant positive correlation ($PCCs = 0.843$, $R^2 = 0.711$) between CN_{pcf} and *CZ*. The content of coarse aggregates in the dominant structure did not exhibit monotonic related to anti-rutting performance of the asphalt mixture. Therefore, an optimum aggregate content of 57% was utilized. The Mann-Whitney *U* test revealed that the mesoscale skeleton structure of the asphalt mixes before and after rutting exhibited excellent stability. This study further indicated the applicability of combining CN_{pcf} to adjust the mix design to enhance the rutting resistance of asphalt mixture and to prevent rutting expansion in flexible pavement.

1. Introduction

As a direct object of various traffic loads and damage medium, the damage resistance of asphalt pavement significantly determines the performance of the road. With the growth of traffic volume, heavy overload and channelized traffic conditions, the probability of damage to asphalt pavement is greatly increased, which not only impacts the serviceability of the road, but also causes potential safety threats to the road traffic. Therefore, in order to improve the damage resistance of pavement, prolong its service life and enhance its performance, the demand for the structural and functional design of asphalt pavement has increased.

The primary load-bearing part of asphalt mixture is the internal skeleton structure [1,2]. A robust skeleton structure generally endows asphalt mixture with good deformation resistance, which is typically reflected in its rutting resistance under high temperature conditions [3]. The internal skeleton structure of skeleton-dense conventional mixture is categorized on the basis of two main indicators, VCA_{mix} (percent voids in coarse mineral aggregate in asphalt mixtures) and VCA_{drc} (percent voids in coarse mineral aggregate in the dry rodded condition). However, for convenience of engineering applications, these two metrics simplify the complexity of the mesoscale structural state of coarse aggregate particles [4,5]. Asphalt mixture is a typical multi-phase granular material composed of aggregates and asphalt binder, and its mechanical response depends largely on the skeletal stability of aggregates and the properties of asphalt binder [6]. Specifically, the stability of skeleton structure for coarse aggregates is most vital for the deformation resistance of asphalt mixtures, because it provides the mixture with internal friction and load-bearing capacity to resist the stresses induced by the traveling loads [7,8]. Continuity of *meso*-skeleton structure can enrich the chain of transmission of force in asphalt mixtures and alleviate stress concentration [9]. Therefore, it is important to

* Corresponding authors.
E-mail addresses: niudongyu_1984@chd.edu.cn, niudongyu_1984@163.com (D. Niu), niuyh@chd.edu.cn (Y. Niu).

https://doi.org/10.1016/j.conbuildmat.2023.131784
Received 19 November 2022; Received in revised form 10 April 2023; Accepted 12 May 2023
Available online 26 May 2023

increase the strength of the internal skeleton structure of the asphalt mixture system and enhance the continuity of the skeletal force chain at the mesoscale level, which urgently requires further investigation of the design method and discrimination basis of the mesoscale skeleton structure.

Typical gradation design methods for asphalt mixture have been for a significant period and the associated research is relatively well-established. The principal methods are the maximum packing density curve method [10] (i.e., Fuller's method), Superpave method [11], Bailey's method [12], stone asphalt concrete (SAC) method [13], and so on. Although these methods offer distinct advantages during application, the mainstream grading design methods typically aim to establish a denser macroscopic skeletal structure on a volumetric scale. This goal is pursued in order to enhance the overall performance of the asphalt mixture, with greater skeletal density being associated with improved resistance to various forms of distress. However, major of gradation design methods have inherent deficiencies in optimizing the contact state for the skeletal structure, which hinders the enhancement of asphalt mixture performance [14–16]. Moreover, disturbing aggregates have some negative effect on the continuity of the skeleton structure, which cannot be ignored. Therefore, it is essential to consider aggregates that disturb the skeletal continuity for the optimal design of mesoscale skeleton.

Mathematical representation is an essential method to analyze the characteristics of mesoscale skeleton formed by coarse aggregates. The current leading approach for skeleton characterization is based on particle packing theory. This theory evaluates the contact and disruption of internal particles in each grade of aggregates, and characterizes the range of sieve sizes of aggregates that contribute to the mechanical response of asphalt mixture. Kim et al., [17] found that the void ratio is a suitable criterion for evaluating the inter-contact between coarse aggregates in asphalt mixture. This criterion based on the necessary conditions for the particles to contact each other in soil mechanics, and it provides the proper deformation and cracking resistance for asphalt mixture. Subsequently, Guarin et al., [15] proposed a novel method for determining the coarse aggregates that constitute the skeleton structure. They defined the dominant aggregate size range (DASR), which constitutes the dominant skeleton structure for bearing load forces in asphalt mixture. The void ratio of DASR can be used to evaluate the performance of asphalt mixture. Numerous results of gradations and indoor asphalt mixture tests indicate that the void ratio of DASR is a key parameter to evaluate the aggregate embedding structure and the rutting resistance of asphalt mixture. With deep knowledge of the disturbing aggregate undermining effect, Guarin et al., [18] proposed the Disruption Factor by taking into account the global disruption caused by the internal contact of the asphalt mixture. With this, the first study was carried out for the effect of disturbing aggregates. Along with to the awareness of three-dimensional packing and filling theory, more accurate characterization studies of multi-level skeletal structures were gradually derived to avoid the one-sidedness and subjectivity of two-dimensional packing and filling theory [19–22], which further extended the DASR framework to a sensible extent.

Subsequently, Yideti et al., [23] and Lira et al., [24] launched an in-depth exploration of the optimal design of the skeletal structure of asphalt mixes based on asphalt concrete skeleton structure (AFSS). Various experiments were carried out to verify the relationship between the optimal design of the skeleton structure and the deformation resistance of asphalt mixes, and it was also proposed to control the content of coarse aggregates in appropriate levels to ensure better performance. Furthermore, the application of particle packing theory in concrete has been developed and extended effectively [25]. Chu et al., [26–28] conducted studies by investigating the effect of continuous filling of voids between particles, and integrated the analysis of aggregate particle packing system with slurry water film. The study revealed the law of wet packing under continuous filling, which in turn significantly enhanced the performance of concrete. The application of particle accumulation theory in construction materials has been extended more abundantly. In summary, numerous studies have quantitatively evaluated the disruptive effect of disturbing aggregates on the skeleton structure by means of particle accumulation theory. The necessity of a well embedded multi-stage structure for forming the *meso*-skeleton structure has been fully verified. However, the quantification characterization criterion of disturbing aggregates for the asphalt mixes with dominant skeleton structure is not reliable sufficiently, and the influence of disturbing aggregates on the mesoscale skeletal properties of asphalt mixes is not comprehensively characterized. Moreover, there are few studies that combined disturbing aggregates with contact coordination effect to investigate their corresponding influence on the mixture skeletal structure and rutting resistance performance.

Digital image processing (DIP) techniques have been widely applied in many research areas, and the application of DIP technology for skeleton structure analysis is well developed [29–31]. In view of the natural differences in grayscale distribution of asphalt mixture, its structural characteristics [32] can be extracted by suitable filtering [33,34] and segmentation [34,35]. Along with the basic aggregate state, the reasonable estimation of the contact state for the aggregate skeleton enables optimization of the analysis accuracy. Coenen et al., [34] proposed the utilization of the harmonic function to characterize the aggregate orientation distribution while analyzing the two-dimensional images of the mixture. Moreover, they adopted the surface distance threshold (SDT) to define the contact state between the aggregates, which occurred when the surface pixel distance of the aggregates was less than SDT. Sefidmazgi et al., [36] suggested that the aggregate contact state can be characterized using the indicators of proximity length, aggregate contact number, contact area and contact plane orientation, and established relationships with the macroscopic performances of asphalt mixture. Shi and Wang et al., [9,37,38] introduced qualitative and quantitative evaluation criteria for the formation of desired skeleton structure by the coarse aggregates. Wang et al., [39] revealed that the gradation type affected the average number of contact points of the asphalt mixture significantly, while the contact direction was independent of the gradation type. The results of indirect tensile strength and fatigue tests showed that the short-term and long-term mechanical properties of the mixture were both directly influenced by the contact properties of the aggregates.

Given the above background, this paper focused on the characteristics of mesoscale skeleton structure for asphalt mixture. The coordination number of particle contact force (CN_{pcf}) was proposed as an indicator to characterize the contact properties of mesoscale skeleton. DIP technology and rutting test were combined to quantitatively evaluate the negative effects of disturbing aggregates on the stability of skeleton structure of asphalt mixture from mesoscale to macroscale. Moreover, the effect of CN_{pcf} on the rutting resistance of asphalt mixture was investigated. The results of this work provided an innovative approach for the material design and evaluation of asphalt mixture.

2. Materials and methods

2.1. Materials and properties

In this study, the performance of the base asphalt (Table 1) used to

Table 1
Asphalt performance parameters.

Type of asphalt	Performance Parameters		Indicators
Karamay 70#	Penetration(25℃, 5 s, 100 g)/0.1 mm		66
	Ductility(15℃, 5 cm/min)/cm		>100
	Softening point /℃		50.5
	RTFOT	Quality loss/%	−0.512
		Penetration Ratio/%	71
		Residual Ductility/cm (15℃, 5 cm/min)	20

make the asphalt mixture is tested according to the specification JTG E20-2019 [40]. All aggregates are obtained from locally produced limestone in Shaanxi Province, China. The density properties of each grade of aggregates which were used to form the asphalt mixture specimens are shown in Table 2.

2.2. Gradation design and calculation

2.2.1. Gradation design method

The performance of asphalt mixture can be significantly affected by the key sieve passage rate, When the key sieve determined by nominal maximum aggregate size (NMAS) are 2.36 mm and 4.75 mm, the aggregate in this portion carried the majority of the load on the asphalt mixture. Aggregates with the break-even size from 2.36 mm to 4.75 mm significantly affect the skeleton structure, which can be considered as the primary sensitive particle size [41]. Furthermore, aggregates with particle size above 4.75 mm contribute the most to stabilize the skeleton, while aggregates from 2.36 mm to 4.75 mm contribute less to the contact points, which leads to insufficient stability of the skeleton structure [18]. The coarse aggregate particles can reach the tightest contact state when the percentage of the finer components (i.e., 4.75 mm to 9.5 mm) in coarse aggregate was 60% [42]. Zhang et al., [43] indicated that the contribution of 4.75 mm and 2.36 mm sieved aggregates to the load resistance was more than 50%. Niu [44] selected the proportions of 2.36 mm to 4.75 mm as 0%, 5%, 10%, and 15%, respectively, and found that the road performance and mechanical properties of the mixture were worse at their contents of 0% and 15%.

In view of this, this paper refers to the SAC design theory and selects 4.75 mm and 2.36 mm as the control sieves, and designs 9 types of gradations of asphalt mixture by orthogonal combination with different skeleton structure characteristics, the calculation processes are shown in section 2.2.2.

2.2.2. Calculation of gradation

In this section, the values of control sieve and disturbing aggregate content are selected in section 2.2.1 and the complete gradation curves are obtained by substituting into Eqs. (1) and (2). Table 3 exhibits the details of the various gradations as well as optimum asphalt content (OAC), and all the gradation curves are shown in Fig. 1.

$$\begin{cases} P_1 = a\left(\dfrac{d_1}{D_{\max}}\right)^b \\ P_2 = a\left(\dfrac{d_2}{D_{\max}}\right)^b \end{cases} \tag{1}$$

$$P_{Di} = a\left(\frac{D_i}{D_{\max}}\right)^b \tag{2}$$

where D_i is the coarse aggregate sieve diameter, mm; P_{Di} is the passage rate of D_i sieve, %; $D_{\max}$ is the maximum particle size of mineral, mm; P_1 is the passage rate of the nominal maximum particle size, %; P_2 is the passage rate of 4.75 mm sieve, %; d_1 is the nominal maximum particle size, mm; d_2 is 4.75 mm; a and b are coefficients.

2.2.3. Experimental methodology

To investigate the effect of disturbing aggregate content on the performance of asphalt mixture with high temperature rutting resistance, the Marshall test and the rutting test were carried out in this paper according to the specification JTG E20-2019 [40] for 9 types of asphalt mixture with different structures designed in the section 2.2. The Marshall specimens and standard rutting plates were produced by the compaction method and wheel rolling method, respectively. Among them, 5 Marshall specimens and 3 rutting plates were prepared for each gradation. The Marshall stability was used as the basic evaluation indicator of asphalt mixture, and the high-temperature rutting test under standard conditions (60℃) was used to evaluate the high temperature rutting resistance of asphalt mixture.

3. Analysis of the dominant skeleton of asphalt mixture and coarse aggregate contact characteristics

The relative content of coarse and fine aggregates in the asphalt mixture determines whether the internal system of the asphalt mixture can form a well embedded structure. Neither can interact independently in any case and form a well embedded network structure to resist external loads. And the damage to the skeleton structure caused by disturbing aggregates cannot be underestimated. Therefore, it is essential to develop an appropriate model to evaluate the desired distribution of coarse and fine aggregates in the asphalt mixture in order to induce better nested combinations.

The contact state of coarse aggregates can be mathematically characterized by contact parameters, which contributes to further investigations of the mechanism for optimal design of the mesoscale skeleton. For the purpose of investigating the relationship between coarse aggregate contact parameters and the mesoscale contact state of coarse aggregate in mixture, this section proposes accurate coarse aggregate contact parameters, establishes a criterion for evaluating whether coarse aggregate is in dense contact, and analyzes them based on digital image processing techniques.

3.1. Asphalt mixture dominant skeleton analytical method

3.1.1. Particle identification method of the dominant skeleton

The number of aggregate contact zones (*CZ*) that can be generated by each singular particle varies in the dense nested packing formed by particle filling, i.e., different coordination numbers [23]. The coordination number is a reflection of the contact state between the particles [45,46], so as to achieve a stable and regular dense filling, only four typical packing methods are commonly utilized, respectively, simple cubic, oblique square, wedge-shaped tetrahedral and rhombohedron [47]. By filling and arranging the spheres, the parameters related to the spheres and voids can then be obtained for varying regular patterns of arrangement [48].

In asphalt mixture, the enhancement of skeletal continuity provides significantly improved resistance to permanent load deformation [9]. When *CZ* are insufficient, the skeletal continuity state is constrained and contact forces may concentrate at the partial contact points and cause cracks in the mixture. Hence, the identification of the contact state between particles on adjacent sieve is critical.

The weighted average void diameter, d_{avg}, of adjacent sieve sizes, according to the assumption of equal volume and three-dimensional packing theory, is used to analyze the contact state between particles under different packing patterns [19].

Since sieve size D_2 is only the minimum particle size of this grade of aggregate, and the maximum particle size of this grade of aggregate is the previous sieve size D_1, it cannot adequately characterize the volume of aggregate by calculating the packing volume of the two adjacent

Table 2
Relative density of each grade of aggregates.

Particle size (mm)	13.2	9.5	4.75	2.36	1.18	0.6	0.3	0.15	0.075
Apparent relative density	2.817	2.763	2.736	2.683	2.685	2.673	2.667	2.657	2.625
Gross volume relative density	2.789	2.73	2.709	2.634	2.637	2.619	2.603	2.584	2.567

Table 3
Gradation and optimum asphalt content.

Gradation	Passing Ratio (%)										OAC (%)
	16	13.2	9.5	4.75	2.36	1.18	0.6	0.3	0.15	0.075	
R54S050	100.0	97.5	76.6	46.0	41.0	26.9	17.8	11.6	7.6	5.0	4.76
R54S075	100.0	97.5	76.6	46.0	38.5	25.5	17.1	11.4	7.5	5.0	4.60
R54S100	100.0	97.5	76.6	46.0	36.0	24.2	16.4	11.1	7.4	5.0	4.44
R57S050	100.0	97.5	74.9	43.0	38.0	25.3	17.0	11.3	7.5	5.0	4.67
R57S075	100.0	97.5	74.9	43.0	35.5	23.9	16.3	11.0	7.4	5.0	4.55
R57S100	100.0	97.5	74.9	43.0	33.0	22.6	15.6	10.7	7.3	5.0	4.42
R60S050	100.0	97.5	73.2	40.0	35.0	23.7	16.2	10.9	7.4	5.0	4.58
R60S075	100.0	97.5	73.2	40.0	32.5	22.3	15.5	10.6	7.3	5.0	4.48
R60S100	100.0	97.5	73.2	40.0	30.0	20.9	14.7	10.3	7.2	5.0	4.38

***NOTE*:** R54 in R54S050 means 54% of the aggregate above 4.75 mm, while S050 means 5% of the aggregate between 2.36 mm and 4.75 mm.

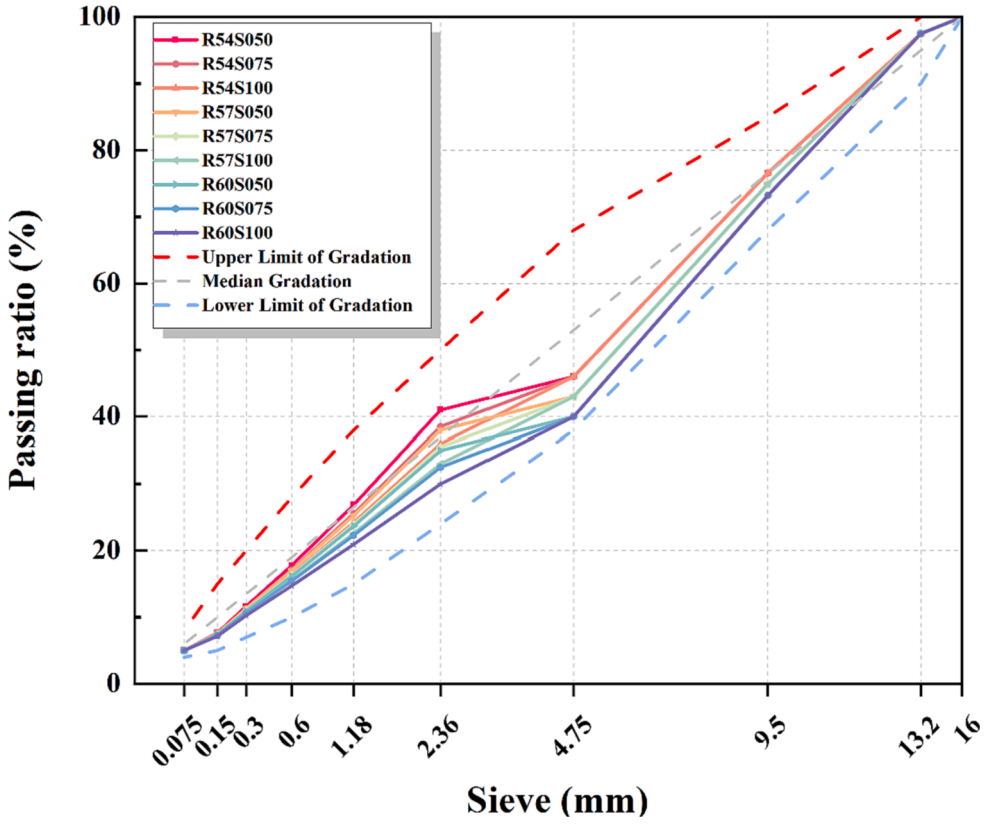

Fig. 1. Asphalt mixture gradation curve for this research.

grades of aggregate with sieve size. Consequently, in this section, the characteristic particle size [49], d_i, is chosen instead of d_{avg}. For any sieve, the calculation of the d_i is shown in Eq. (3).

$$\lg(d_i) = [\lg(D_1) + \lg(D_2)]/2 \tag{3}$$

The particle size of the aggregate forming the predominant skeleton structure can be determined as follows:

(1) When the particles on D_1 are packed as a simple cubic, the pile shows the maximum void ratio and the least number of particle contact points, which yields a maximum weighted average void diameter as D_{max}, refer to Eq. (4).

$$D_{max} = \frac{1.1 \times d_{i1} d_{i2}}{\sqrt[3]{d_{i1}^3 + 2.36 \times d_{i2}^3}} \tag{4}$$

(2) When the particles on D_1 are packed as rhombohedron, the pile exhibits the lowest void ratio and the maximum number of particles contact points, which yields a minimum weighted average void diameter as D_{min}, as shown in Eq. (5).

$$D_{min} = \frac{1.1 \times d_{i1} d_{i2}}{\sqrt[3]{d_{i2}^3 + 2.36 \times d_{i1}^3}} \tag{5}$$

(3) When the screening rate of the particles on D_1 and D2 sieves are φ1 and φ2, respectively, the weighted average void diameter between particles is $d_{w,avg}$ in this case, as given in Eq. (6)

$$d_{w,avg} = 0.732 \times d_{i1} d_{i2} \sqrt[3]{\frac{\varphi_1 + \varphi_2}{\varphi_1 d_{i2}^3 + \varphi_2 d_{i1}^3}} \tag{6}$$

(4) Integrating Eqs. (4) to (6), the identification for the particle size range of the aggregates for dominant skeleton can be obtained, see Eq. (7).

$$\frac{1.1 \times d_{i1} d_{i2}}{\sqrt[3]{d_{i2}^3 + 2.36 \times d_{i1}^3}} \leqslant d_{w,avg} \leqslant \frac{1.1 \times d_{i1} d_{i2}}{\sqrt[3]{d_{i1}^3 + 2.36 \times d_{i2}^3}} \tag{7}$$

Where d_{i1} and d_{i2} are the characteristic particle sizes obtained when D_1 and D_2 act as the minimum particle size for a given grade of

aggregate, respectively.

3.1.2. Analysis of the particle size range for the dominant skeleton

The inter-granular contact effect is crucial for load transfer and dispersion, while the capacity of load transfer is related highly and positively to the square of the particle size [50]. The skeleton structure is primarily composed of coarse aggregates, where the larger the particle size is, the greater the load carrying capacity is [41]. Considering this, the primary object of skeleton analysis in this paper is the coarse aggregate of mixture which mainly bears and transmits the load.

The delineation of coarse and fine aggregates is defined by the nominal maximum particle size (NMPS) [12] and the delineating of the break-even sieve size for the control sieve can be calculated by Eq. (8). The NMPS of the gradations in this paper is 13.2 mm, then the primary control sieve (*PCS*) is approximately 2.904 mm. As the range of aggregate particle sizes on the 2.36 mm sieve is 2.36 mm to 4.75 mm, the range of particle sizes used for the dominant skeleton analysis is 2.36 mm to 16 mm, i.e., the range of values of D_2.

$$PCS = 0.22 \times NMPS \tag{8}$$

The characteristic particle sizes of the aggregates for each grade can be calculated according to Eq. (6), and they are shown in Table 4. The coarse aggregate skeleton structure of the gradations R54S050 to R60S100 was analyzed by the method in Section 3.1.1, as shown in Fig. 2 below.

(1) When $D_2 \geq 9.5$ mm, as in Fig. 2(a). The $d_{w,avg}$ of all gradations are lower than D_{min}, that is because the voids formed by the accumulation of aggregates on 13.2 mm sieve in the gradation are too narrow to accommodate all the aggregates on 9.5 mm sieve, thus the aggregates with particle size in the range of 9.5 mm ~ 16 mm are unable to form a well-contacted skeleton structure, which do not belong to particles for the dominant skeleton structure.
(2) When $D_2 = 4.75$ mm, as in Fig. 2(b). The $d_{w,avg}$ of all the gradations meet the requirements of Eq. (7), which indicates that the voids formed by the accumulation of aggregates on the 9.75 mm sieve in the gradation can accommodate the particles on the 4.75 mm sieve. Thus, the aggregate with particle size range of 4.75 mm ~ 13.2 mm can be assessed as particles for the dominant skeleton structure.
(3) When $D_2 = 2.36$ mm, as in Fig. 2(c). The $d_{w,avg}$ of all gradations are larger than D_{max}, that is due to the excessive aggregate on 2.36 mm sieve in the gradation, which is partially filled in the void formed by the accumulation of aggregates on 4.75 mm sieve to develop a well-contacted skeleton, but the surplus aggregates would burst the skeleton and reduce the contact points. Thus, the aggregate with particle size range of 2.36 mm ~ 9.5 mm cannot be identified as particles for the dominant skeleton structure.

3.2. Contact coordination parameters for the coarse aggregates of the dominant skeleton

According to the analysis results of the dominant skeleton, the mineral mixture can be classified into oversized structure (OS), dominant structure (DS), secondary structure (SS). The aggregates of the secondary structure are filled in the void formed by the DS, as shown in Fig. 3(a).

In the secondary structure (SS), aggregates less than 0.225 times of the minimum particle size, i.e., *D*, of the dominant structure (DS) will merely fill the skeleton structure of the mixture [49], as shown in Fig. 3 (b). Conversely aggregate with particles larger than 0.225*D* will disrupt the complete continuity of the skeleton structure, as shown in Fig. 3(c).

Consequently, in this section, such particles are defined as disturbing aggregate (DA). Since the maximum nominal particle size of the aggregate is varied, the corresponding particle size range of the disturbed particles is also different [49]. The classifications of the internal structure and its particle size range for asphalt mixture in this study are presented in Table 5.

Based on the studies of Chun [18,51] and Yideti [23], this paper defines the corresponding key indicators of asphalt mixture with dominant skeleton structure, including the total volume value of the mixture (V_T), the effective volume value of the dominant structure mixture (V_T^{DS}), the volume value of oversized structure (V_{agg}^{OS}), the volume value of the dominant structure (V_{agg}^{DS}), the volume value of the secondary structure (V_{agg}^{SS}), and the volume value of the disturbing structure (V_{agg}^{SSDA}), and so on, as shown in Fig. 4.

According to the volumetric parametric relationship and combined with the corresponding key indicators, the void volume ratio of the dominant skeleton structure particles (η_{DS}) is defined as the ratio of the sum of the V_{agg}^{SS} and *VMA* over the V_T^{DS}, as shown in Eqs. (9) and (10).

$$V_T^{DS} = V_T - V_{agg}^{OS} \tag{9}$$

$$\eta_{DS} = \frac{V_V^{DS}}{V_T^{DS}} = \frac{V_{agg}^{SS} + VMA}{V_T - V_{agg}^{OS}} \tag{10}$$

The ratio of the V_{agg}^{SSDA} over the V_T^{DS} is defined as the volume ratio of disturbing particles (η_{SSDA}), given in Eq. (11).

$$\eta_{SSDA} = \frac{V_{agg}^{SSDA}}{V_T - V_{agg}^{OS}} \tag{11}$$

The embedded structures formed by particle filling correspond to different coordination numbers respectively, which can reflect the interaction state between particles, following the studies of Scott and Bernal et al., [45,46] on random filling of equal size spherical particles with different sizes as well as its skeleton structure. Yideti et al., [23] established a theoretical mathematical relationship between theoretical voids and coordination number by means of particle coordination number to characterize the state of primary chain for contact between particles.

Based on the above theory and the relationship equation of coordination number [23], the parameter that represents the contact state of coarse aggregates, i.e., CN_{pcf} is proposed in this paper by considering the effect of the volume of disturbing particles on the dominant skeleton particle contact. Following the formulation of the coordination number [23], the correction of the volume effect for disturbing aggregates is introduced to it. Thus, the parameter, CN_{pcf}, is calculated by Eq. (12).

$$CN_{pcf} = 2.827 \times \left(\frac{\eta_{SSDA}}{\eta_{DS}} \times 100\%\right)^{-1.069} \tag{12}$$

From Eq. (12), the CN_{pcf} can be calculated from the gradations in the paper, as shown in Table 6 below.

3.3. Acquisition and validation of the contact coordination parameters

With varying grayscale distributions [52], asphalt mixture can be separated from different components to accurately characterize the internal structure by digital image processing (DIP) techniques. Given this, this section investigates the contact characteristics of aggregates for dominant structure in asphalt mixture through DIP techniques to verify the feasibility of CN_{pcf}. The processes of extracting the contact characteristics for the dominant aggregates in this section can be grouped into three parts: image acquisition, image processing, and contact analysis.

Table 4
The characteristic particle size of each grade of aggregates.

Sieve (mm)	16	13.2	9.5	4.75	2.36
D_1 (mm)	19	16	13.2	9.5	4.75
D_2 (mm)	16	13.2	9.5	4.75	2.36
d_i (mm)	17.44	14.53	11.20	6.72	3.35

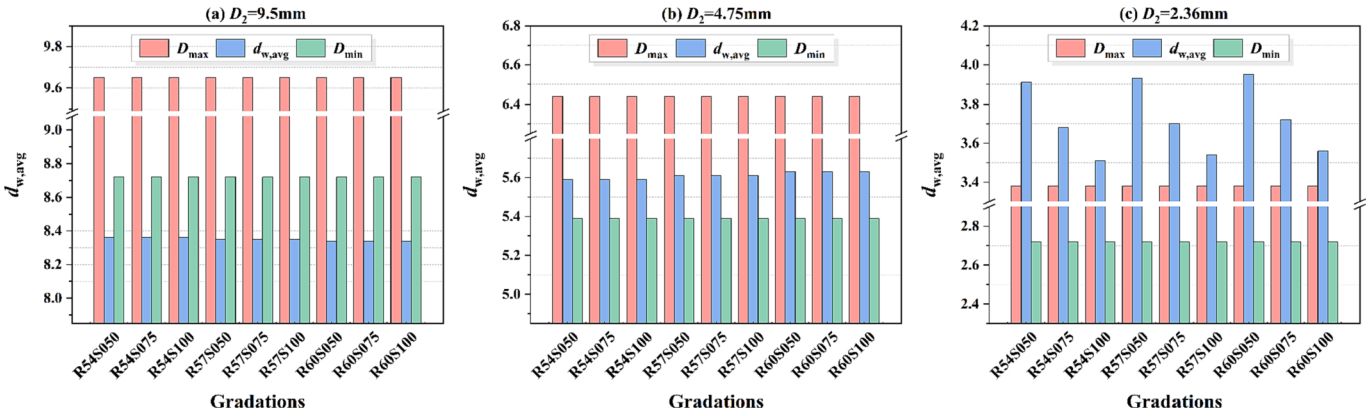

Fig. 2. Weighted average void diameter of adjacent coarse aggregate sieves.

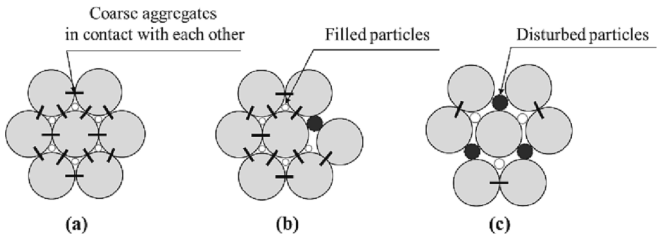

Fig. 3. Example of the particle contact status [15].

Table 5
The control sieve and particle size range of each structure.

Structure division	Control sieve (mm)	Particle size range (mm)
OS	13.2	13.2 ~ 16
DS	9.5, 4.75	4.75 ~ 13.2
SS	2.36, 1.18, 0.6, 0.15, 0.075	0 ~ 4.75
DA	2.36, 1.18	1.18 ~ 4.75

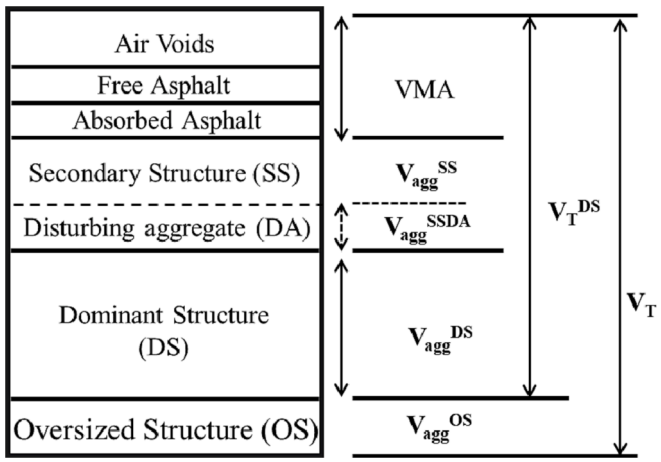

Fig. 4. The volume composition of asphalt mixture.

3.3.1. Digital image-based contact condition acquisition

(1) Image acquisition

As shown in Fig. 5(a), each specimen in this section was divided into three slices, with four original image samples and two rutting image samples obtained after high-precision photographing. A total of 18 images were captured for each gradation, and altogether 162 images were accessed, which met the requirements of test accuracy [53]. Note here that the surface of the specimen slices after cutting is muddy, and each slice need to be cleaned and placed at the room temperature for several hours to ensure that the cut surface is dry to avoid the residual moisture from affecting the accuracy of image acquisition.

As the technical requirements of two-dimensional digital image processing for photographic quality, a 10-megapixel CCD-camera (CE100-30GM/C) from Hikvision was utilized to capture the slices. the image acquisition system is shown in Fig. 5(b), including specimen slices, CCD-camera, aperture and image acquisition software.

Table 6
Coordination numbers of particle contact force for each gradation.

Gradation	Asphalt/aggregate ratio (%)	*VV* (%)	*VMA* (%)	η_{DS} (%)	η_{SSDA} (%)	CN_{pcf}
R54S050	4.76	3.9	14.7	59.55	23.10	7.78
R54S075	4.60	4.0	14.6	59.62	24.69	7.26
R54S100	4.44	4.1	13.7	59.18	26.01	6.81
R57S050	4.67	4.1	14.4	55.96	21.33	7.93
R57S075	4.55	4.2	14.1	55.88	22.85	7.35
R57S100	4.42	4.3	14.2	56.10	24.52	6.85
R60S050	4.58	4.2	13.9	52.14	19.53	8.08
R60S075	4.48	4.3	14.8	52.78	21.40	7.42
R60S100	4.38	4.4	14.4	52.65	22.94	6.87

(2) Image processing

In this paper, a co-processing strategy of independent Python programming and iPAS-2 software is adopted. Firstly, a Python program was applied for image pre-processing according to the Scikit-Image library, and then a multi-process script was implemented by Python to manipulate the iPAS-2 [34,54] software for *CZ* extraction aiming to optimize the data processing efficiency. Finally, a suitable data purification program was also designed to obtain information on *CZ* of the aggregates for dominant skeleton. As shown in Fig. 5(c), the key image processing procedures included Grayscale transformation, *Hmax* filtering, Median filtering, Threshold-value filtering, Watershed algorithm, and Binarization. After the execution of the program, each identified and separated aggregate would be serialized and its coordinate data in the image would be collected to facilitate the identification of contact conditions.

(3) Contact analysis

In the pattern of DIP of aggregates, the contact judgment between any aggregates would be transformed into a particular threshold distance. If the distance between the two is narrower than a predefined

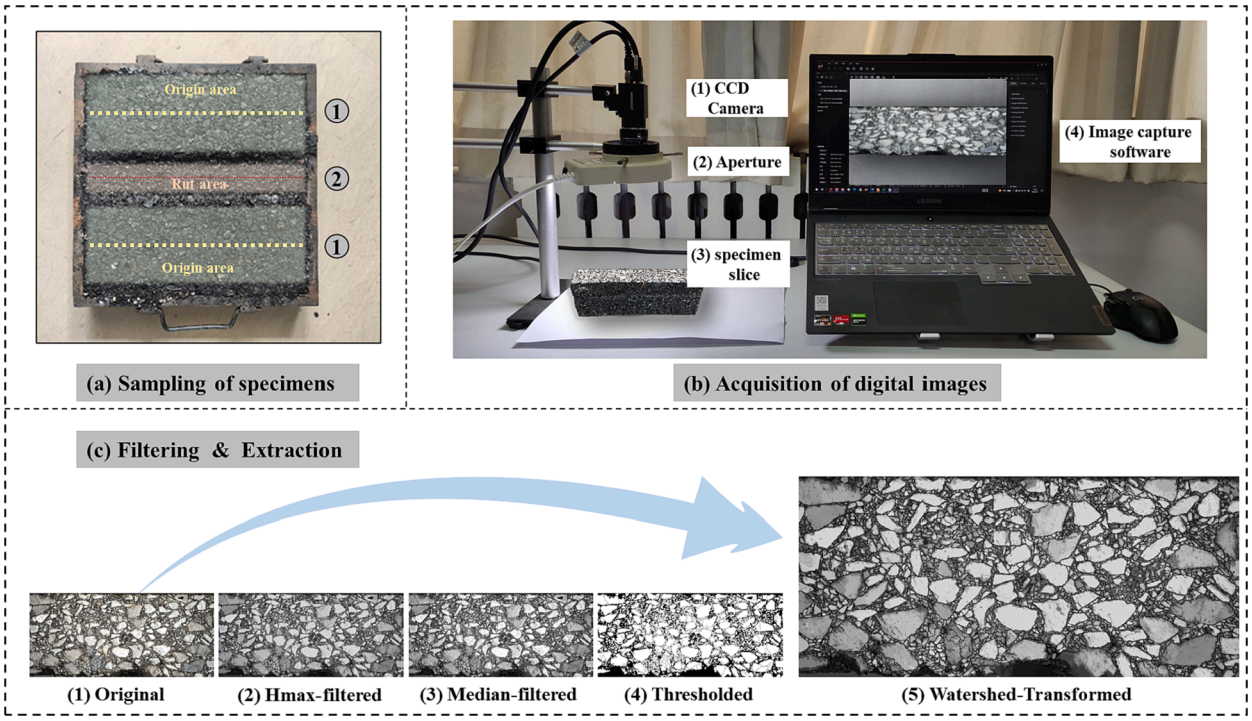

Fig. 5. Aggregate cross-section image acquisition and data processing.

threshold value, the aggregates are considered as pairwise contact [55]. According to the results of the dominant skeleton analysis in Section 3.1, the minimum analyzed particle size is adopted as 4.75 mm, while the contact threshold is 0.23 times of the minimum analyzed particle size, i.e., 1.0925 mm. For instance, the number of *CZ* is 3, when aggregate #1 is in contact with #2, #3, and #4, respectively, as shown in Fig. 6.

3.3.2. Validation of the contact coordination parameters for coarse aggregate

The relationship between the number of *CZ* for aggregates above 4.75 mm and CN_{pcf} parameter in asphalt mixture is shown in Fig. 7. An increase in the number of *CZ* indicates that the continuity of the internal contact of the mixture is enhanced, which expands the transfer path of internal stresses. The two exhibited a highly positive correlation in statistical level with $PCCs = 0.843$ and $R^2 = 0.711$, which indicated that the contact coordination parameters for coarse aggregate could characterize the internal skeletal contact state of the mixture effectively.

Also, it can be found that, on the one hand, under the conditions of constant percentage of aggregates above 4.75 mm, the number of *CZ* significantly decreases with the addition of sensitive aggregates from 2.36 mm to 4.75 mm, which is attributed to the destruction of the contact skeleton by sensitive aggregates. Moreover, the larger the proportion of sensitive aggregates, the stronger the destructive effect is, which exhibits a decrease in the number of *CZ*. On the other hand, the number of *CZ* is increased as the proportion of sensitive aggregates from 2.36 mm to 4.75 mm remained constant, with the developing proportion of aggregates above 4.75 mm. It is attributed to the improvement for the probability of adjacent contact of aggregates by the increasing number of the aggregates for dominant structure, which shows an enlargement of the number of *CZ*.

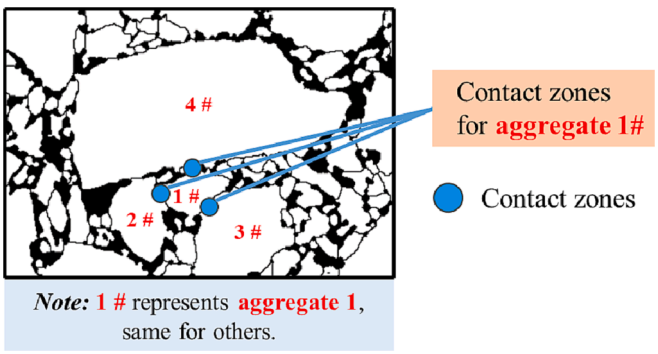

Fig. 6. An example of contact identification.

4. Influence of contact coordination parameters for coarse aggregates on the rutting resistance of asphalt mixture

4.1. Contact coordination parameters and performance of asphalt mixture

(1) Marshall stability

The Marshall stability of each gradation has been indicated in Table 7. The Marshall stability of the asphalt mixture increases with the variation of the CN_{pcf}, showing a sharp rise and then a gradual decrease. When the CN_{pcf} are around 7.4, the stability of the mixture is relatively better and the mechanical properties are optimal; meanwhile, with the CN_{pcf} less than 7.2, the stability is relatively low. But it still meets the requirement of MS $\geq$ 8kN according to the specification, which indicates that the basic mechanical properties of the asphalt mixture designed in this study can be ensured.

Nevertheless, it needs to be emphasized that, as shown in Fig. 8(a), with the increase in the proportion of sensitive aggregates of 2.36 mm to 4.75 mm from 5% to 10%, the decrease in Marshall stability raises significantly, which indicates that the sensitive aggregate content is excessive and the surplus sensitive aggregate disrupts the skeleton structure. When the sensitive aggregate content is in between, i.e., the CN_{pcf} is from 7.2 to 7.6, the embedded contact of the aggregates for dominant structure increases and the voids of the dominant structure can be densely filled.

On the other hand, the stability is relatively greater for the percentage of aggregates above 4.75 mm at 54%. In the scope of this paper,

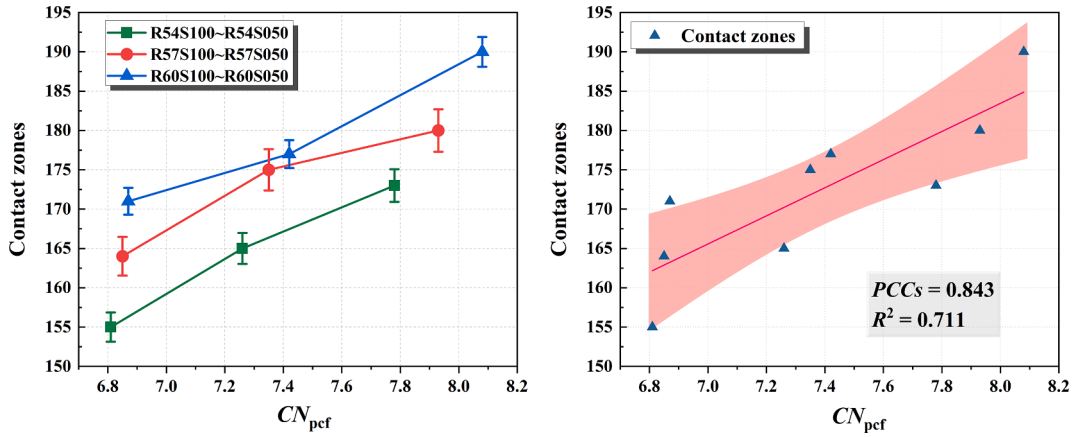

Fig. 7. Tendency of aggregate contact coordination parameters with CZ.

Table 7
Marshall stability and dynamic stability of each gradation.

Gradation	Asphalt/Aggregate ratio (%)	CN_{pcf}	Marshall Stability (kN)	Dynamic Stability (Times/mm)
R54S050	4.76	7.78	11.78	1029
R54S075	4.60	7.26	12.44	1514
R54S100	4.44	6.81	9.70	912
R57S050	4.67	7.93	11.12	1349
R57S075	4.55	7.35	11.64	1676
R57S100	4.42	6.85	9.83	1129
R60S050	4.58	8.08	10.95	1055
R60S075	4.48	7.42	11.21	1425
R60S100	4.38	6.87	9.49	962

with respect to the mechanical performance of asphalt mixture, a lower proportion of aggregates above 4.75 mm corresponds to a relatively lower CN_{pcf} and a greater stability as well as better mechanical performance of the asphalt mixture.

(2) Dynamic stability

In this study, the rutting test results are shown in Table 7, and all the dynamic stability of the various levels of CN_{pcf} meet the basic requirement of $DS \geq 800$ times/mm according to the specification. As shown in Fig. 8(b), the dynamic stability of the asphalt mixture exhibited an increasing and then decreasing trend with the CN_{pcf} enlarged, meanwhile the rutting depth varied oppositely. It is indicated that the degree of embedded contact between the aggregates for dominant structure is the critical factor to determine the capability of the asphalt mixture for resisting permanent deformation at high temperature. The CN_{pcf} can effectively characterize the embedded contact state of the aggregates for dominant structure as well as control the high temperature performance of the mixture.

Also, it is to be noted that the average decrease in dynamic stability reaches 9.13% as the proportion of sensitive aggregates of 2.36 mm to 4.75 mm increases from 5% to 10%. This indicates that the sensitive aggregate content is excessive and the surplus sensitive aggregate would disrupt the skeleton structure and affect the embedded contact between aggregates, which reduces the capacity of the skeleton to bear load transfer. When the content of disturbing aggregate is 7.5%, the mixture achieves the optimal condition for resisting rutting.

On the other hand, the dynamic stability was relatively maximum when the percentage of aggregates above 4.75 mm reached 57%. Compared with the gradation R60S050 and R54S050, the dynamic stability of R57S050 was increased by 27.87% and 23.72%, respectively; while compared with the gradation R60S075 and R54S075, the dynamic stability of R57S075 was increased by 14.98% and 9.67%, respectively; whereas compared with the gradation R60S100 and R54S100, the dynamic stability of the gradation R57S100 was improved by 14.79% and 19.22%, respectively. As a result, there is an optimal proportion of aggregates above 4.75 mm for improved high-temperature stability of

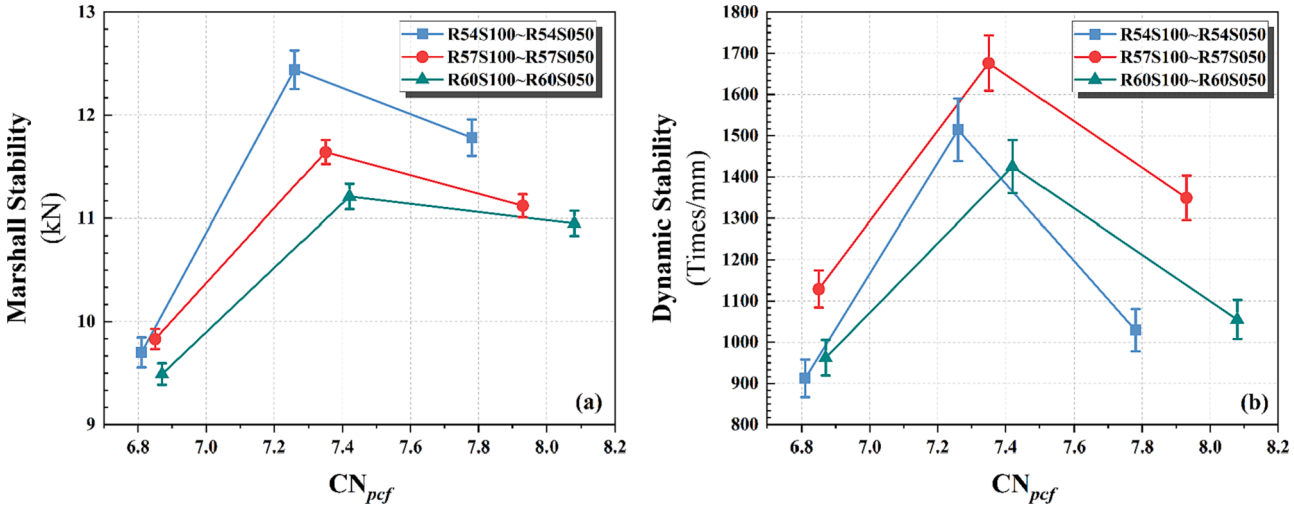

Fig. 8. Tendency of Marshall Stability and Dynamic Stability.

asphalt mixture within this paper, which can facilitate a more optimal embedded contact of the aggregates for dominant structure and enhance the resistance of the skeleton structure to deformation.

4.2 Contact coordination parameters and characteristics of rutting resistance

High-temperature rutting is one of the irreversible diseases for asphalt mixture. Once the rutting occurs, its effect lasts for the entire life-cycle of the pavement and indirectly increases the probability of developing other diseases. Given this, it is necessary to quantify the structural properties of asphalt mixture before and after rutting test to evaluate the performance of asphalt mixture for rutting resistance, although the asphalt mixture exhibits reasonable mechanical properties during the experimental phase.

In this section, the contact characteristics of the asphalt mixture before and after the rutting test were considered in a comprehensive assessment. Based on the methodology in the Section 3 of this paper, the *CZ* were extracted from un-rutted samples and rutted samples. Taking into account that *CZ* is the direct information that can be obtained from the image, the parameter CN_{pcf} is a mathematical abstract representation of the contact characteristics for the coarse aggregates. It has been verified in this study that the two are highly correlated, and adopting the *CZ* value in the test stage can simplify the complexity of the analysis. The contact zone distribution characteristics of the control and test groups are shown in Fig. 9.

By statistical analysis, the average probability density of the number of $CZ \geq 3$ among all levels of the mixture was 61.39% under the original state without testing. After the rutting test, the majority of the asphalt mixture showed an increasing trend in the number of *CZ*. Meanwhile, the average probability density of $CZ \geq 3$ was 65.18%. From the mesoscale level, this is due to the displacement of the originally dispersed individuals or the aggregates for skeleton with fewer *CZ* under the load, which is reflected as deformation in the macroscopic sense.

For the characterization of *CZ* within the mixture, the average coordination number is preferred and its calculation is shown in Eq. (13):

$$\overline{n}_c = \frac{1}{m}\sum_{i=1}^{m} n_c^i \tag{13}$$

where $\overline{n}_c$ is the average coordination number of aggregates, m is the total number of aggregates, and n_c^i is the number of *CZ* of the aggregate *i*.

The stability of the skeleton structure before and after the test indicates the performance level of the mixture to resist rutting. As shown in Table 8 and Fig. 10, the mixture has greater resistance of damage when the content of the aggregates for dominant structure is 57%, and the rate of variation for $\overline{n}_c$ before and after the test is the lowest.

Furthermore, the rate of variation of the gradation R60S075 is negative. Even though the mixture itself exhibits greater dynamic stability, the analysis of the mesoscale contact shows that there is already a variation within the structure, resulting in the decrease of the contact coordination number, which negatively affects the long-lasting rutting resistance.

Table 8
The magnitude of coordination number variation.

Gradation	Average coordination number ($\overline{n}_c$)		Variation rate (%)
	Original	Rutted	
R54S050	2.758	2.920	5.89%
R54S075	2.560	2.694	5.23%
R54S100	2.717	2.868	5.54%
R57S050	3.241	3.392	4.67%
R57S075	3.113	3.203	2.88%
R57S100	2.987	3.117	4.36%
R60S050	2.891	3.062	5.93%
R60S075	2.784	2.691	**−3.33%**
R60S100	2.838	2.992	5.41%

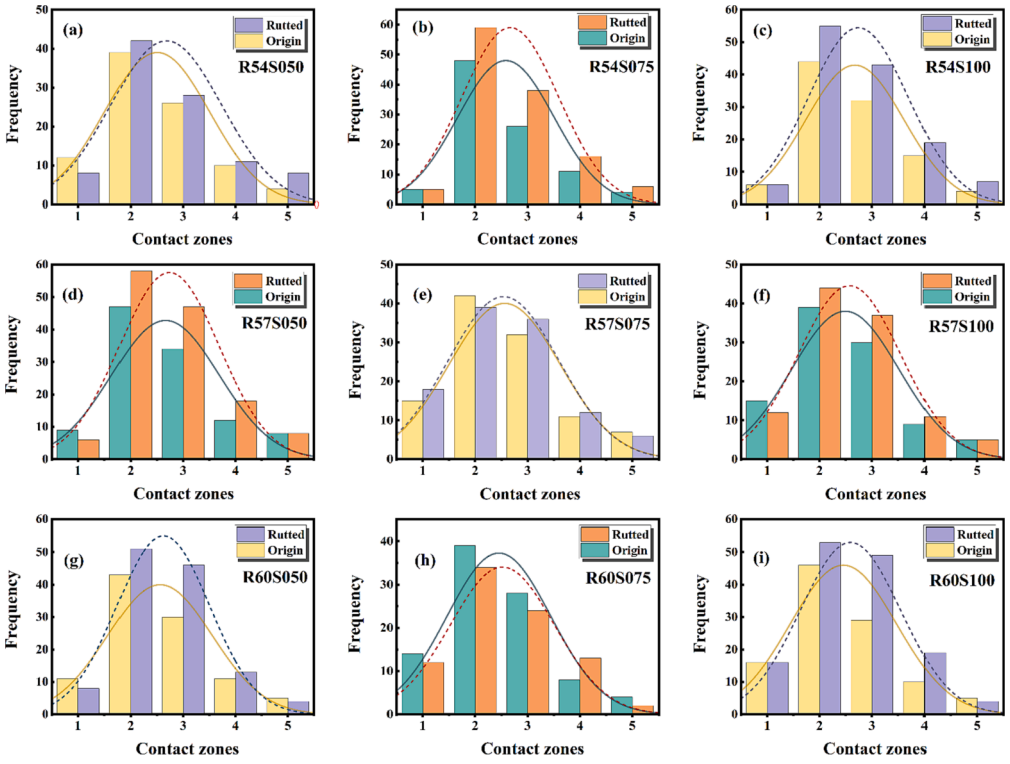

Note: The curves are fitted normal distributions.
Where the solid line is the original sample, and the dashed line is the sample after rutting test.

Fig. 9. Variation of the frequency of aggregate CZ before and after rutting test. From (a) to (i) correspond to the gradations of R54S050 to R60S100 respectively.

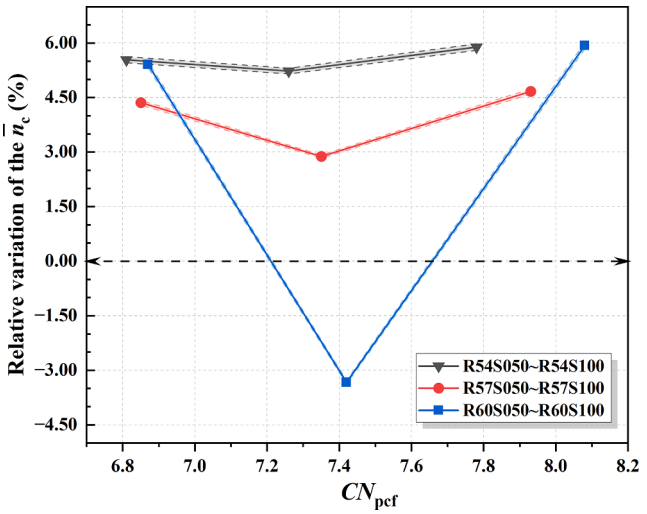

Fig. 10. The variation of aggregate coordination number before & after rutting test.

Nevertheless, it is important to be aware that not all "displacements" lead to further deepening of the damage. The *Mann-Whitney U* test [56] is capable for estimating whether two groups of samples are statistically homogeneous, thereby serving the purpose of distinguishing if the distributions are similar. To clarify the discrepancy in the distribution of *CZ* inside the asphalt mixture before and after rutting test, the *Mann-Whitney U* test with a significance level of $\alpha = 0.01$ was applied to evaluate the degree of variation.

As shown in Table 9, the contact zone distributions of all levels of asphalt mixture in this study remained significantly similar before and after the rutting test, and there was a large *P*-value to demonstrate the excellent performance of this asphalt mixture in resisting rutting. Such results further indicate that the contact coordination parameters for coarse aggregate are reasonable for optimizing the rutting resistance of asphalt mixture.

5. Conclusions and future work

In this study, the influence of contact characteristics of aggregates inside the asphalt mixture on its rutting resistance was investigated by adopting the parameter CN_{pcf} to characterize the structural conditions of the dominant structure. The relationship between CN_{pcf} and the contact conditions of the dominant structure was identified, and the influence of CN_{pcf} on the resistance of asphalt mixture to high-temperature rutting was investigated. Based on the results of this study, the following conclusions can be drawn:

(1) Upon analyzing the gradation design based on CN_{pcf} through Python script combined with image sampling, it was discovered that the majority of aggregates exhibited CZ with values greater than 3, while the number of suspended particles was minimal. The coarse aggregates were found to be embedded in intimate contact with each other, thereby forming a mesoscale skeletal structure.

(2) With the increase in value of CN_{pcf}, the number of *CZ* and $\overline{n}_c$ of the mixture tended to increase, particularly when the content of coarse aggregate was constant. The correlation of the number of *CZ* and $\overline{n}_c$ with CN_{pcf} was significant ($PCCs = 0.843$, $R^2 = 0.711$), which demonstrated that CN_{pcf} could effectively characterize the contact between aggregates inside the mixture.

(3) It was found that the Marshall stability and dynamic stability first increased and then decreased with the variation of the CN_{pcf}, which indicated that the optimum value of the dominant structure can be determined. Furthermore, considering the NMAS was 13.2 mm in this study, the asphalt mixture can achieve higher performance level with 43% aggregate content on the break-even sieve of 4.75 mm.

(4) *CZ* number of asphalt mixture with almost all gradations increased after the rutting test, and the particles with $CZ \geq 3$ in all gradations occupied the majority. When the content of aggregates for dominant structure was 57% and the percentage of disturbing aggregates was 7.5%, the corresponding mixture possessed outstanding rutting resistance.

(5) Through the Mann-Whitney *U* test at the significance level $\alpha = 0.01$, it was evident that the asphalt mixture designed in this study can achieve better resistance to rutting deformation. It was further demonstrated that the CN_{pcf} is valuable for guiding the performance optimization of asphalt mixture in the design period.

Table 9
Verification of similarity of aggregate contact distribution before & after rutting test ($\alpha = 0.01$).

Gradation	*Z*-value	*P*-value
R54S050	−1.02995	0.30453
R54S075	−0.72012	0.47375
R54S100	−0.47296	0.63591
R57S050	−0.73021	0.46613
R57S075	0.03596	0.97107
R57S100	−0.66323	0.50838
R60S050	−0.7346	0.46352
R60S075	−0.50612	0.61963
R60S100	−1.34259	0.17943

In summary, an optimized design parameter (CN_{pcf}) based on particle accumulation theory was proposed and reliably verified. The influence of CN_{pcf} was analyzed on the rutting resistance of asphalt mixture. In future work, because the CN_{pcf} was mainly investigated in the mixture type of AC-13, its feasibility of mathematical representation still needs to study for other types of asphalt mixture. Meanwhile, the influence of the angular properties to the aggregates was not considered much in this paper. Thus, the morphology of aggregates will be thoroughly studied.

CRediT authorship contribution statement

Dongyu Niu: Methodology, Writing – original draft, Supervision. **Weibo Shi:** Methodology, Writing – original draft, Data curation. **Chen Wang:** Investigation, Writing – review & editing. **Xiwang Xie:** Investigation, Writing – review & editing. **Yanhui Niu:** Supervision, Methodology.

Declaration of Competing Interest

The authors declare that they have no known competing financial interests or personal relationships that could have appeared to influence the work reported in this paper.

Data availability

Data will be made available on request.

Acknowledgements

The research is supported by the National Natural Science Foundation of China (No. 51608045), Science and Technology Project of Housing and Urban Rural Development Department of Shaanxi Province (2020-K11), Fundamental Research Funds for the Central Universities, Chang'an University, China (Nos. 300102310301, 300102311404).

References

[1] M. Fang, D. Park, J.L. Singuranayo, H. Chen, Y. Li, Aggregate gradation theory, design and its impact on asphalt pavement performance: a review, Int. J. Pavement Eng. 20 (12) (2019) 1408–1424, https://doi.org/10.1080/10298436.2018.1430365.

[2] Y.Q. Tan, M. Guo, Interfacial thickness and interaction between asphalt and mineral fillers, Mater. Struct. 47 (4) (2014) 605–614, https://doi.org/10.1617/s11527-013-0083-8.

[3] S. Li, X.W. Wang, X.P. Ji, J.Y. Li, K. Li, J.K. Shi, Investigating the rutting mechanism of asphalt mixtures based on particle tracking technology, Constr. Build. Mater. 260 (2020) 10, https://doi.org/10.1016/j.conbuildmat.2020.119781.

[4] H. Azari, R. McCuen, K. Stuart, The effect of vertical inhomogeneity on compressive properties of asphalt mixtures, J. Assoc. Asphalt Paving Technol. 73 (2004) 121–145.

[5] Y. Peng, L.J. Sun, Micromechanics-based analysis of the effect of aggregate homogeneity on the uniaxial penetration test of asphalt mixtures, J. Mater. Civ. Eng. 28 (11) (2016) 10, https://doi.org/10.1061/(asce)mt.1943-5533.0001634.

[6] X.Y. Zhu, Influence of interfacial zone between asphalt mastic and aggregate on the elastic behavior of asphalt concrete, Constr. Build. Mater. 49 (2013) 797–806, https://doi.org/10.1016/j.conbuildmat.2013.08.072.

[7] J. Chen, H. Li, L.B. Wang, J.T. Wu, X.M. Huang, Micromechanical characteristics of aggregate particles in asphalt mixtures, Constr. Build. Mater. 91 (2015) 80–85, https://doi.org/10.1016/j.conbuildmat.2015.05.076.

[8] G.Q. Liu, D.D. Han, Y.L. Zhao, J.P. Zhang, Effects of asphalt mixture structure types on force chains characteristics based on computational granular mechanics, Int. J. Pavement Eng. 23 (4) (2022) 1008–1024, https://doi.org/10.1080/10298436.2020.1784894.

[9] L. Shi, D. Wang, X. Xiao, X. Qin, Meso-structural characteristics of asphalt mixture main skeleton based on meso-scale analysis, Constr. Build. Mater. 232 (2020) 117263.

[10] W.B. Fuller, S.E. Thompson, The laws of proportioning concrete, Trans. Am. Soc. Civ. Eng. 59 (2) (1907) 67–143.

[11] M.W. Witczak, Simple performance test for superpave mix design, Transp. Res, Board, 2002.

[12] W.R. Vavrik, W.J. Pine, G. Huber, S.H. Carpenter, R. Bailey, The Bailey method of gradation evaluation: the influence of aggregate gradation and packing characteristics on voids in the mineral aggregate, J. Assoc. Asphalt Paving Technol. 70 (2001), https://doi.org/10.3181/00379727-118-29893.

[13] Q. Sha, The design and construction of the series of stone asphalt concrete SAC, People's Traffic Publishing House, 2005 in Chinese.

[14] J. Haddock, C. Pan, A. Feng, T. White, Effect of gradation on asphalt mixture performance, Transp. Res. Rec. 1681 (1) (1999) 59–68, https://doi.org/10.1061/(ASCE)MT.1943-5533.0003315.

[15] A. Guarin, Interstitial component characterization to evaluate asphalt mixture performance, University of Florida, 2009.

[16] H.N. Yu, S.H. Shen, G.P. Qian, X.B. Gong, Packing theory and volumetrics-based aggregate gradation design method, J. Mater. Civ. Eng. 32 (6) (2020) 04020110, https://doi.org/10.1061/(asce)mt.1943-5533.0003192.

[17] S. Kim, R. Roque, A. Guarin, B. Birgisson, Identification and assessment of the dominant aggregate size range (DASR) of asphalt mixture, J. Assoc. Asphalt Paving Technol. 75 (2006).

[18] A. Guarin, R. Roque, S. Kim, O. Sirin, Disruption factor of asphalt mixtures, Int. J. Pavement Eng. 14 (5) (2013) 472–485, https://doi.org/10.1080/10298436.2012.727992.

[19] B. Lira, D. Jelagin, B. Birgisson, Gradation-based framework for asphalt mixture, Mater. Struct. 46 (8) (2012) 1401–1414, https://doi.org/10.1617/s11527-012-9982-3.

[20] P.K. Das, B. Birgisson, D. Jelagin, N. Kringos, Investigation of the asphalt mixture morphology influence on its ageing susceptibility, Mater. Struct. 48 (4) (2013) 1–14, https://doi.org/10.1617/s11527-013-0209-z.

[21] B. Lira, D. Jelagin, B.R. Birgisson, Binder distribution model for asphalt mixtures based on packing of the primary structure, Int. J. Pavement Eng. 16 (2) (2015) 144–156, https://doi.org/10.1080/10298436.2014.937713.

[22] Y.H. Dinegdae, I. Onifade, D. Jelagin, B. Birgisson, Mechanics-based top-down fatigue cracking initiation prediction framework for asphalt pavements, Road Mater. Pavement Des. 16 (4) (2015) 907–927, https://doi.org/10.1080/14680629.2015.1055335.

[23] T.F. Yideti, B. Birgisson, D. Jelagin, A. Guarin, Packing theory-based framework for evaluating resilient modulus of unbound granular materials, Int. J. Pavement Eng. 15 (8) (2013) 689–697, https://doi.org/10.1080/10298436.2013.857772.

[24] B. Lira, J. Ekblad, R. Lundström, Evaluation of asphalt rutting based on mixture aggregate gradation, Road Mater. Pavement Des. 22 (5) (2021) 1160–1177, https://doi.org/10.1080/14680629.2019.1683061.

[25] S.H. Chu, Development of infilled cementitious composites (ICC), Compos. Struct. 267 (2021), 113885, https://doi.org/10.1016/j.compstruct.2021.113885.

[26] S.H. Chu, J.J. Chen, L.G. Li, P.L. Ng, A.K.H. Kwan, Roles of packing density and slurry film thickness in synergistic effects of metakaolin and silica fume, Powder Technol. 387 (2021) 575–583, https://doi.org/10.1016/j.powtec.2021.04.029.

[27] S.H. Chu, W.L. Lam, L. Li, C.S. Poon, Packing density of ternary cementitious particles based on wet packing method, Powder Technol. 405 (2022), 117493, https://doi.org/10.1016/j.powtec.2022.117493.

[28] S.H.C. Anderson, Volume-based concrete mix design, ACI Mater. J. 120 (1) (2023) 243–256, https://doi.org/10.14359/51737295.

[29] J. Hu, P.F. Liu, D.W. Wang, M. Oeser, Y.Q. Tan, Investigation on fatigue damage of asphalt mixture with different air-voids using microstructural analysis, Constr. Build. Mater. 125 (2016) 936–945, https://doi.org/10.1016/j.conbuildmat.2016.08.138.

[30] J. Hu, P.F. Liu, D.W. Wang, M. Oeser, Influence of aggregates' spatial characteristics on air-voids in asphalt mixture, Road Mater. Pavement Des. 19 (4) (2018) 837–855, https://doi.org/10.1080/14680629.2017.1279072.

[31] T.S. Li, P.F. Liu, C. Du, M. Schnittcher, J. Hu, D.W. Wang, M. Oeser, Microstructural analysis of the effects of compaction on fatigue properties of asphalt mixtures, Int. J. Pavement Eng. 23 (1) (2022) 9–20, https://doi.org/10.1080/10298436.2020.1728532.

[32] Z. Du, J. Yuan, Q. Zhou, C. Hettiarachchi, F. Xiao, Laboratory application of imaging technology on pavement material analysis in multiple scales: a review, Constr. Build. Mater. 304 (3) (2021), 124619, https://doi.org/10.1016/j.conbuildmat.2021.124619.

[33] J. Youtcheff, M.E. Kutay, E. Arambula, N. Gibson, Three-dimensional image processing methods to identify and characterise aggregates in compacted asphalt mixtures, Int. J. Pavement Eng. 11 (6) (2010) 511–528, https://doi.org/10.1080/10298431003749725.

[34] A.R. Coenen, M.E. Kutay, N.R. Sefidmazgi, H.U. Bahia, Aggregate structure characterisation of asphalt mixtures using two-dimensional image analysis, Road Mater. Pavement Des. 13 (3) (2012) 433–454, https://doi.org/10.1080/14680629.2012.711923.

[35] H.G. Brandes, J.G. Hirata, An automated image analysis procedure to evaluate compacted asphalt sections, Int. J. Pavement Eng. 10 (2) (2009) 87–100, https://doi.org/10.1080/10298430801916866.

[36] N.R. Sefidmazgi, P. Teymourpour, H.U. Bahia, Effect of particle mobility on aggregate structure formation in asphalt mixtures, Road Mater. Pavement Des. 14 (sup2) (2013) 16–34, https://doi.org/10.1080/14680629.2013.812844.

[37] L.W. Shi, D.Y. Wang, C.N. Jin, B. Li, H.H. Liang, Measurement of coarse aggregates movement characteristics within asphalt mixture using digital image processing methods, Meas. 163 (2020) 13, https://doi.org/10.1016/j.measurement.2020.107948.

[38] L.W. Shi, Z. Yang, D.Y. Wang, X. Qin, X. Xiao, M.K. Julius, Gradual meso-structural response behaviour of characteristics of asphalt mixture main skeleton subjected to load, Appl. Sci. 9 (12) (2019) 2425, https://doi.org/10.3390/app9122425.

[39] F. Wang, Y. Xiao, P.D. Cui, T. Ma, D.L. Kuang, Effect of aggregate morphologies and compaction methods on the skeleton structures in asphalt mixtures, Constr. Build. Mater. 263 (2020) 11, https://doi.org/10.1016/j.conbuildmat.2020.120220.

[40] JTG E20-2019 Standard test methods of bitumen and bituminous mixtures for highway engineering, Ministry of Transport of the People's Republic of China, 2019.

[41] J.S. Chen, M.C. Liao, Evaluation of internal resistance in hot-mix asphalt (HMA) concrete, Constr. Build. Mater. 16 (6) (2002) 313–319, https://doi.org/10.1016/S0950-0618(02)00037-5.

[42] Y. Hong, H. Zhang, Study of distribution characteristics of aggregate contacts in AC20 HMA based on digital image processing, J. Build. Mater. 14 (001) (2011) 66–70, https://doi.org/10.3969/j.issn.1007-9629.2011.01.014.

[43] Y. Zhang, T. Ma, M. Ling, X.M. Huang, Mechanistic sieve-size classification of aggregate gradation by characterizing load-carrying capacity of inner structures, J. Eng. Mech. 145 (9) (2019), https://doi.org/10.1061/(ASCE)EM.1943-7889.0001640.

[44] D. Niu, Study on performance of asphalt mortar and framework structured asphalt mixture based on meso-mechanics, Chang'an University. (2015).

[45] G.D. Scott, Packing of equal spheres, Nature 188 (4757) (1960) 908–909, https://doi.org/10.1038/188908a0.

[46] J.D. Bernal, J. Mason, Packing of spheres: co-ordination of randomly packed spheres, Nature 188 (4754) (1960) 910–911, https://doi.org/10.1038/188910a0.

[47] L. Fraser, I. Part, systematic packing of spheres: with particular relation to porosity and permeability, J. Geol. 43 (8) (1935) 785–909, https://doi.org/10.2307/30058420.

[48] A.J. Cooke, R.K. Rowe, Extension of porosity and surface area models for uniform porous media, J. Environ. Eng. 125 (2) (1999) 126–136, https://doi.org/10.1061/(asce)0733-9372(1999)125:2(126).

[49] C. Xing. Mesostructure and stress strain transfer mechanism of skeleton filling system of asphalt mixture, Harbin Institute of Technology. 2019.

[50] Y.L. Zhao, T. Xu, X.M. Huang, Z.D. Li, Gradation design of the aggregate skeleton in asphalt mixture, J. Test. Eval. 40 (7) (2012) 1071–1076, https://doi.org/10.1520/jte20120142.

[51] S. Chun, K. Kim, B. Park, J. Greene, Evaluation of the effect of segregation on coarse aggregate structure and rutting potential of asphalt mixtures using dominant aggregate size range (DASR) approach, Ksce. J. Civ. Eng. 22 (1) (2018) 125–134, https://doi.org/10.1007/s12205-017-1372-5.

[52] H. Liang, Investigation of anti-cracking asphalt mixture based on mesomechanical property, South China University of Technology, 2019.

[53] W. Wu, D. Wang, X. Zhang, Z. Li, Research on voids in coarse aggregate of asphalt mixtures with digital image processing and probability statistics, J. Tongji University (Natural Science Edition) 38 (12) (2010) 1792–1795, https://doi.org/10.3969/j.issn.0253-374x.2010.12.015.

[54] Y.H. Yang, H.B. Wang, Y. Yang, H.Z. Zhang, Evaluation of the evolution of the structure of cold recycled mixture subjected to wheel tracking using digital image

processing, Constr. Build. Mater. 304 (2021) 12, https://doi.org/10.1016/j.conbuildmat.2021.124680.
[55] N.R. Sefidmazgi, L. Tashman, H. Bahia, Internal structure characterization of asphalt mixtures for rutting performance using imaging analysis, J. Assoc. Asphalt Paving Technol. 81 (2012) 109–137.
[56] H.B. Mann, D.R. Whitney, On a test of whether one of two random variables is stochastically larger than the other, Ann. Math. Stat. 18 (1) (1947) 50–60, https://doi.org/10.1214/aoms/1177730491.